Astron. Astrophys. 169, 63–70 (1986)

ASTRONOMY AND ASTROPHYSICS

VLA and 100-m telescope observations of two giant galaxies: 0634-20 and 3C445 (2221-02)

P.P. Kronberg[1], **R. Wielebinski**[2], **and D.A. Graham**[2]

[1] Department of Astronomy, University of Toronto, 60 St. George St., Toronto M5S1A7, Canada
[2] Max-Planck-Institut für Radioastronomie, Auf dem Hügel 69, D-5300 Bonn 1, Federal Republic of Germany

Received August 19, 1985; accepted July 10, 1986

Summary. Multifrequency radio maps of total radio power and linear polarization are described and analyzed for giant, southern hemisphere sources, 0634-20 and 3C445. These comprise Effelsberg 100-m telescope and VLA maps made at a total of 5 different frequencies. At 1.4 and 10.6 GHz we have comparable angular resolution and thus can investigate the spectrum over nearly a decade in frequency. We have measured the linear polarization at all the frequencies. The resulting ambiguity-free Faraday rotation maps over each source permit us to place upper limits to the non-relativistic electron density in and around the extended radio lobes. Both sources are suitable as two of the first reliable probes of arcminute-scale variations of the Faraday rotation in our Galaxy. For 0634-20, which extends over 15′ in a zone of moderately high galactic Faraday rotation, we are able to establish that the galactic RM varies by less than 4% over 7′, and by $\lesssim$25% over the entire 15′ extent of 0634-20.

The morphology and spectral index distributions provide strong evidence for *in situ* acceleration in the outer heads, at 300–350 kpc in projection from both galaxy nuclei.

The spectral index of 3C445 is found to steepen *transverse* to the source's long axis, whereas there is little spectral index change *along* the source's long axis. Our analysis of 3C445 suggests that relativistic electrons "age" away from the source axis, where they are no longer accelerated. It is also shown how more detailed, future analyses of the type presented in this paper could lead to the first determination of the unknown, and hitherto elusive "k" factor for relativistic particle populations.

Key words: galaxies – radio observations – active galaxies

1. Introduction

In this paper we present multifrequency radio observations of two large radio sources which have large north-south angular extent and have not previously been studied in detail because of their low declinations. 0634-20 is identified with an elliptical galaxy at $z = 0.056$ (Schilizzi and McAdam, 1975; Danziger et al., 1978), and 3C445 (2221-02) is identified with a $z = 0.0568$ broad-line radio galaxy (cf. Rudy and Tokunaga, 1982). Previous radio maps at 408 MHz by Schilizzi and McAdam (1975) show 0634-20 to extend over 15′, and 3C445 over 10′. These correspond to projected linear dimensions of 0.6 and 0.9 Mpc respectively (for $H_0 = 75$, $q_0 = 0.1$). This places both in the class of very large radio sources. Because our measurements cover an unusually large number and range of frequencies and angular resolution, we are able to search for variations in radio spectral index and Faraday rotation within the large angular dimensions of these two sources.

Apart from the interest in further understanding the physics of very large radio sources, 0634-20 in a zone of high galactic rotation measure at ($l = 230°$, $b = -12°$). This fact, combined with its large angular extent, makes it one of the few individual radio sources which is ideally suited as a probe for small-scale fluctuations in the *galactic* Faraday rotation at moderately low latitudes.

2. The observations and method

2.1. Observational strategy

In order to obtain an unambiguous rotation measure distribution in a zone of relatively high galactic rotation measure, we have obtained total intensity and polarization maps of 0634-20 at several frequencies; $\lambda\lambda$2.8 and 11.1 cm with the Effelsberg 100-m telescope, and $\lambda\lambda$2.0, 6.1 and 20 cm with the NRAO[1] VLA. 3C445, which is at higher galactic latitude ($l = 61\overset{\circ}{.}9$, $b = -46\overset{\circ}{.}7$) and has smaller angular extent, was observed at λ2.8 cm with the 100-m telescope, and at $\lambda\lambda$2, 6.1, and 20 cm with the VLA.

We have also mapped the spectral index over both sources by combining the Effelsberg 2.8 cm maps with the VLA 20 cm maps, after smoothing down the resolution of the latter to the 72″ HPBW of the former. Comparison of these two sets of maps gives several resolution cells over the length of each source, and a wide frequency base of 7.5:1. The VLA was used in its "C" configuration, for which the range of antenna spacings was 70 m to 3.6 km.

By using a filled aperture telescope for the highest frequency maps, our comparison avoids a common problem in comparing low- and high-frequency maps, which is that the interferometer sampling at the highest frequencies sometimes lacks low-order spatial Fourier components. These are crucial for verifying the presence or absence of large-scale emission at the highest frequencies. The radio maps of each source are discussed in turn.

Send offprint requests to: R. Wielebinski

[1] The National Radio Astronomy Observatory is operated by Associated Universities Inc. under contract to the National Science Foundation

Table 1. 10.7 GHz flux and polarization calibrators

Source	Flux [Jy]	Position angle [°]	Polarization [%]
3C 48	2.5	110	6.0
3C 286	4.40	33	11.6

2.2. *Method and calibration*

The 2.8 cm Effelsberg observations were made in 1979 with the 3-horn, 2-channel receiver system (Emerson et al., 1979) in the secondary focus of the 100-m radio telescope. At this frequency the half-power beamwidth (HPBW) is $72'' \pm 2''$. In addition to the beam-switched total intensity channels, data on linear polarization is recorded in the main horn. The reduction procedures are essentially the same as described by Klein and Emerson (1981). Several coverages of the source were obtained in azimuth at different hour angles. They were then added together in order to both reduce the noise and systematic errors in the individual scan baselines. For calibration, we used the sources 3C 48 and 3C 286, with flux density and polarization values as given in Table 1.

The 20 cm VLA observations, along with some limited uv-coverage maps at $\lambda\lambda$6.1 and 2 cm, were made in 1980. The flux density scale and polarization position angle were calibrated using 3C 286 and 3C 138. The phase and instrumental polarization were calibrated using the sources 2227-088 and 0606-223, which lie close to 3C 445 and 0634-20 respectively. The λ20 cm observations of 3C 445 were additionally interspersed with polarization observations of the strongly polarized source, 3C 446. The latter was used as a check against sudden differential ionospheric Faraday rotation which could introduce errors in the λ20 cm polarization maps.

3. Results

3.1. *0634–20*

The 100-m telescope map at λ2.8 cm is shown in Fig. 1. There are long radio "bridges" which extend to each of the outer hotspots, and which are remarkably collinear in structure. The degree of polarization in the bridges varies from $\sim 8\,\%$ to $\sim 30\,\%$. Figure 2 shows the 20 cm VLA map overlaid on the Palomar Sky Survey field which at ($l = 230°$, $b = -12°$) is relatively crowded with stars. The high collinearity is even more striking at this resolution (15″).

Up to a distance of $\sim 3'$ (180 kpc in projection from the galaxy), the degree of polarization at 15″ resolution at λ20 cm is less than 5 % nearly everywhere in the bridge (where the surface brightness is $< 3\,\%$ of peak). At this distance, a transformation occurs, by which the bridge becomes narrower, and the degree of linear polarization suddenly becomes large. Along the 2′ long narrow neck just behind the southern hotspot, the degree of linear polarization is 20–50 %, with relatively constant position angle. A similar "switch" in properties occurs toward the northern hotspot, namely to high degree of polarization at nearly constant angle just at the point where the radio bridge "recollimates" itself into a narrow neck.

The two outer hotspots differ markedly in their linear polarization properties; the northern hotspot is 5 % polarized at its peak and outer edge (at 15″ resolution), whereas the southern

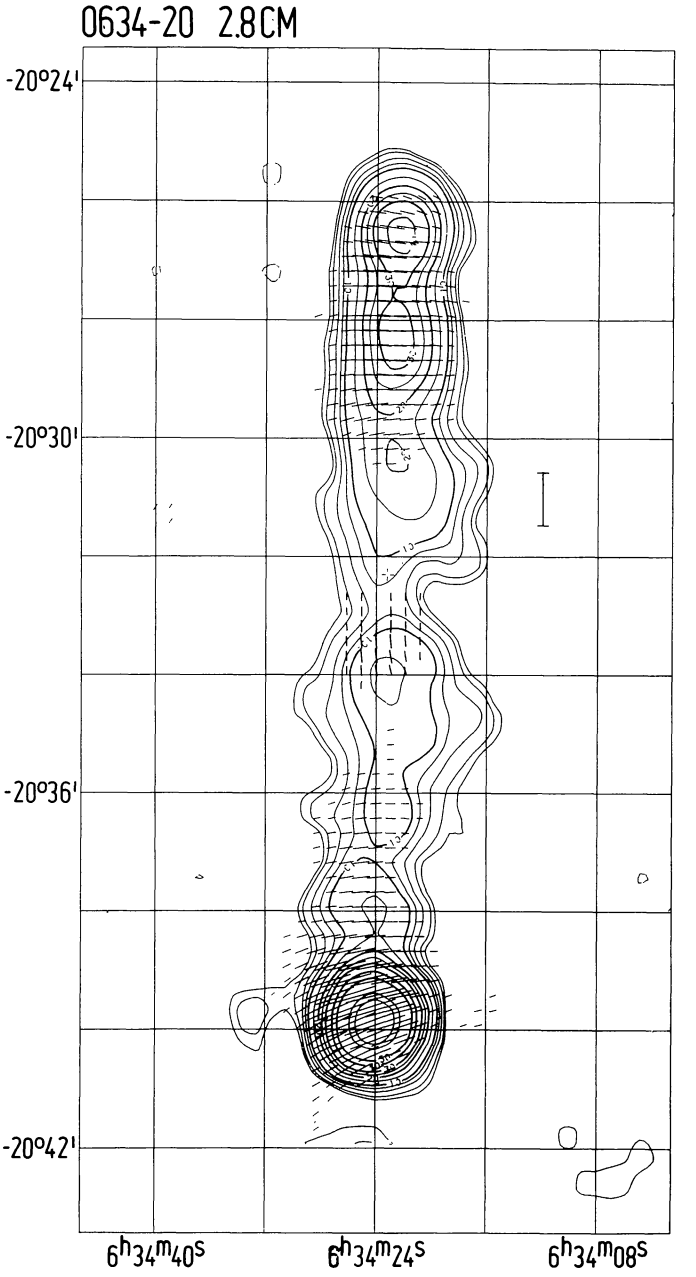

Fig. 1. Radio map of the total intensity of 0634-20 at λ2.8 cm (10.6 GHz) made with the MPIfR 100-m telescope at Effelsberg. The I-map contours are at 15, 20, 30, 40, 75, 100, 125, 150, 200, 250, 375, and 425 mJy/beam. Straight lines indicate the E-vector plane and their lengths are proportional to $\sqrt{Q^2 + U^2}$ such that 1′ equivalent length corresponds to 69 mJy/beam

hotspot is $\sim 20\,\%$ polarized, and has two subregions at position angles differing by 60°. Figure 3a and b contain maps at 4″.5 resolution of the northern and southern hotspot regions, and shows the same difference in polarization degree between the two hotspots. The fact that this difference persists at both 14″ and 4″.5 resolution suggests that, if it is due to beam cancellation of highly polarized sub-parts of the northern hotspot, this must occur on a smaller scale than 4 kpc. One could suppose, on the other hand, that differential Faraday rotation is sufficiently strong in the northern hotspot to cause nearly complete depolarization at

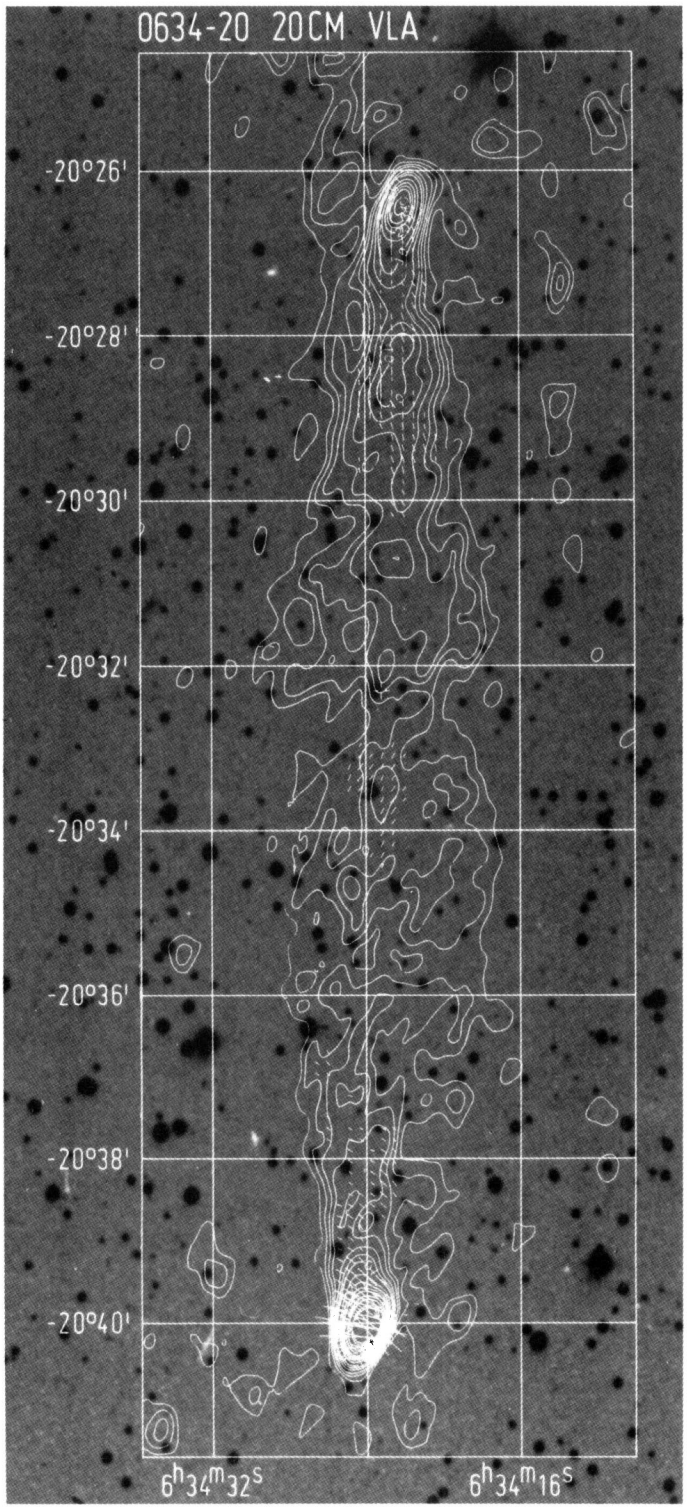

Fig. 2. VLA map of 0634-20 overlaid on the optical field from the Palomar Sky Atlas Survey. The total intensity contours are at 10, 20, 30, 40, 50, 80, 100, 150, 200, 250, 300, 400, 500, 750, and 850 mJy/beam. The polarization lines represent $\sqrt{Q^2+U^2}$ and the *E*-vector orientation. Their lengths are scaled such that 1′ equivalent length corresponds to 273 mJy/beam

λ6.1 cm. This seems unlikely, however, since our rotation measure map at 75″ resolution shows only small changes in Faraday rotation over the entire ~1 Mpc extent of 0634-20. We conclude that the substructure of the two outer hotspots is genuinely different. Maps at yet higher resolution are needed to clarify the difference.

On comparing the λ20 cm VLA map with the λ2.8 cm 100-m map at the latter's resolution, we find no large-scale variations of spectral index between the two frequencies. We emphasize, however, that the resolution of this comparison is not sufficient to detect spectral index variations *transverse* to the source axis, or within the outer hotspot complexes.

Similarly, we compared the polarization distributions at $\lambda\lambda$20 cm (VLA), 11.1 cm, 6.1 cm, and 2.8 cm (all Effelsberg 100-m maps), and show a Faraday rotation measure map of 0634-20 in Fig. 4. This distribution was generated by reducing the resolution of the λ20 cm VLA map in Fig. 2 to 75″, that of the λ2.8 cm Effelsberg map in Fig. 2, and converting the polarization angle differences to the usual units of Faraday rotation measure (RM). The additional maps of Stokes parameters *I*, *Q*, and *U* at $\lambda\lambda$11.1 and 6.1 cm (not shown) were used to eliminate $n \cdot 180°$ ambiguities in determining the RM map. The unusually long frequency "baseline" in Fig. 2 enables us to easily detect very small changes in Faraday rotation across the source, since for $\lambda\lambda$20–2.8 cm, a 1° change in position angle corresponds to a Faraday rotation change of only 0.4 rad m^{-2}.

Figure 4 shows that the RM over 0634-20 deviates by at most 3 rad m^{-2} from a mean of +58 rad m^{-2} over the entire 7′ length of the *southern* portion of the source. Just north of the galaxy there is insufficient polarized signal at both frquencies to reliably determine the RM, but the highly polarized northern bridge, and the head have the same RM to within ~3 rad m^{-2} of +44 rad m^{-2}. Just north of, or at the galaxy centre, the RM appears to increase in step-like fashion by +13 rad m^{-2}. We cannot unambiguously say whether this RM jump occurs near the source, or in our galaxy, however the relatively large mean RM is almost certainly galactic, since several nearby (in *l*, *b*) extragalactic sources also have similarly large, positive RM's (cf. Simard-Normandin et al., 1981).

Comparison of Figs. 2 and 4 shows that the rotation measure of the highly polarized zone (~60% at 20 cm) just south of the galaxy is virtually identical to that of the outer lobe. The fact that this region appears neither Faraday rotated nor depolarized at 20 cm can be used to estimate the magneto-ionic "strength" of the medium at projected distances of 44″ (45 kpc) to 120″ (121 kpc) ($H_0 = 75$) south of the radio galaxy's centre. We assume here that the emission in this region, which is close to maximally polarized at 20 cm, is centered on the radio source axis which also passes through the centre of the galaxy, i.e. that it is not a foreground feature.

The observational requirement that the internal Faraday rotation of this region does not exceed 2 rad m^{-2} and the assumption of an equipartition magnetic field of $3.7\,(1+k)^{+2/7}$ μG require an upper limit on the smoothed-out electron density, $n_e < 5\ 10^{-5}\,(1+k)^{-2/7}$ cm^{-3} (k is the relativistic proton/electron energy ratio). This rather stringent limit lies well below that which produces the levels of X-ray emission observed in clusters of galaxies. It is also surprisingly low in view of the recent discovery by Fosbury et al. (1984) of a small region giving [O III] emission lines at ~20″ (20 kpc) on each side of the galaxy nucleus, since the latter must also be associated with a much higher density of ionized gas. We also note that the very similar rotation measures of regions C and D (Fig. 4) occur *despite the fact that their projected mag-*

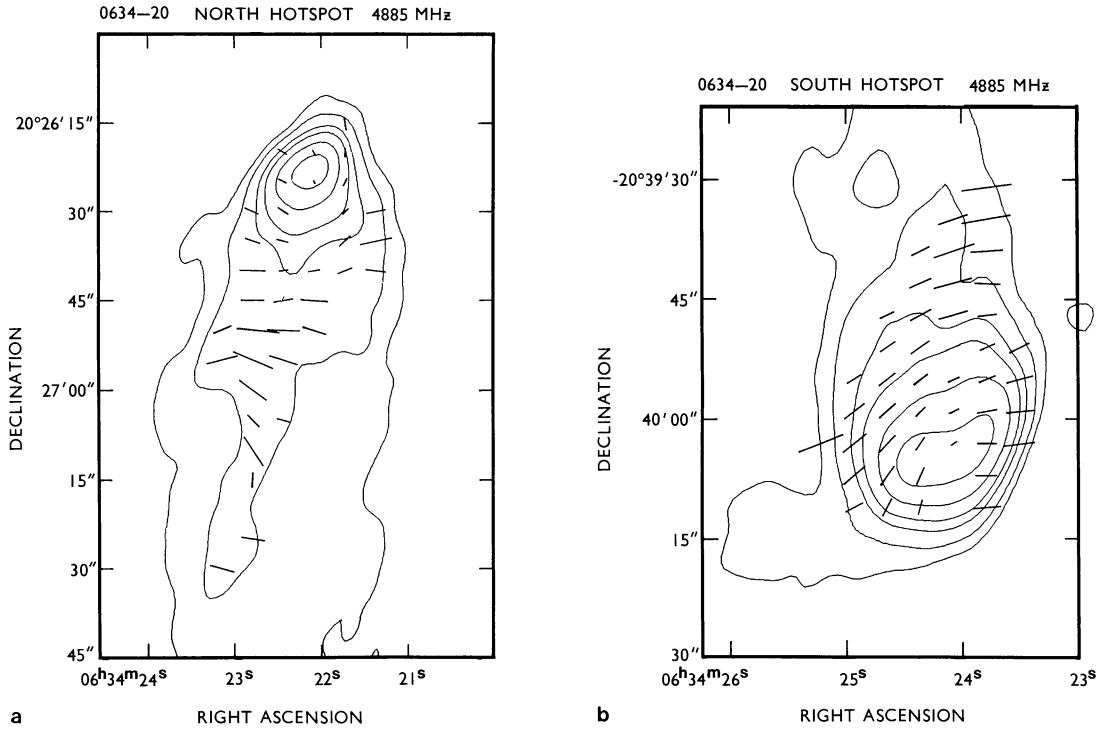

Fig. 3. **a** 4885 MHz VLA map of the northern head of 0634 – 20. Contours are shown at 5 %, 10 %, 20 %, 30 %, 50 %, and 80 % of peak flux, which is 63.1 mJy/beam. The maximum E-vector lines are proportional to percentage of linear polarization such that 5″ equivalent length corresponds to 44 % polarization. The HPBW is 4.5. **b** Comparable map for the southern hotspot, whose peak surface brightness is 115 mJy/beam. The I-contours are at the same intervals as in **a**, and the percentage polarization vectors are scaled such that 5″ equivalent length corresponds to 59 % polarization. The degree of polarization reaches 60–70 % on the west side of the bridge region

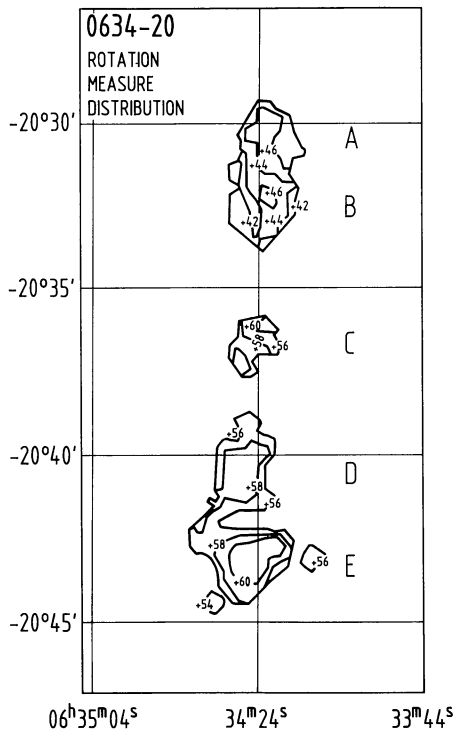

Fig. 4. Distribution of Faraday rotation measure (RM) over 0634-20 at 75″ resolution between $\lambda\lambda$2.8 cm and 20 cm. For this (wavelength)^2 interval a change of 1 rad m^{-1} corresponds to a position angle difference of 2.48

netic fields are highly aligned in orthogonal directions. This fact suggests that very little of the 50–60 rad m^{-2} RM in the southern half of 0634-20 occurs within the radio lobes, since the line-of-sight field component would presumably also change between regions C and D and hence modulate any internally generated RM.

The upper limits (Fig. 4) of Δ(RM)/RM 4 % over 7′ and Δ(RM)/RM < 25 % over 15′ gives important limits on the arcminute-scale foreground galactic RM. Although it is not clear whether the RM jump of ~13 rad m^{-2} immediately north of the galaxy is galactic or extragalactic, 0634-20 provides evidence against differential galactic RM at this latitude on the scale of a few arcminutes. We conclude that, *at least in this* (l, b) *direction*, extended radio sources up to 10′ are unlikely to be depolarized by differential galactic RM across their angular width.

3.2. 3C 445 (2221–02)

Figure 5 shows the λ20 cm VLA map of 3C 445 superimposed on the optical field from the Palomar Sky Atlas Survey. The central radio peak at 22^{h}21^{m}14^s.67, −02°21′26″.3 corresponds to the galaxy nucleus, and there are no other obvious radio-optical associations. At this resolution the northern outer complex appears double, whereas the southern hotspot appears as a single feature. The south-proceeding jet-like feature contains a prominent bright spot at 22^{h}21^{m}15^s.4, −02°22′15″.4, which has a rather low degree of polarization ($\lesssim$8 %) at λ21 cm. This feature is embedded in a wider complex of radio emission whose surface brightness is ~20 mJy/beam.

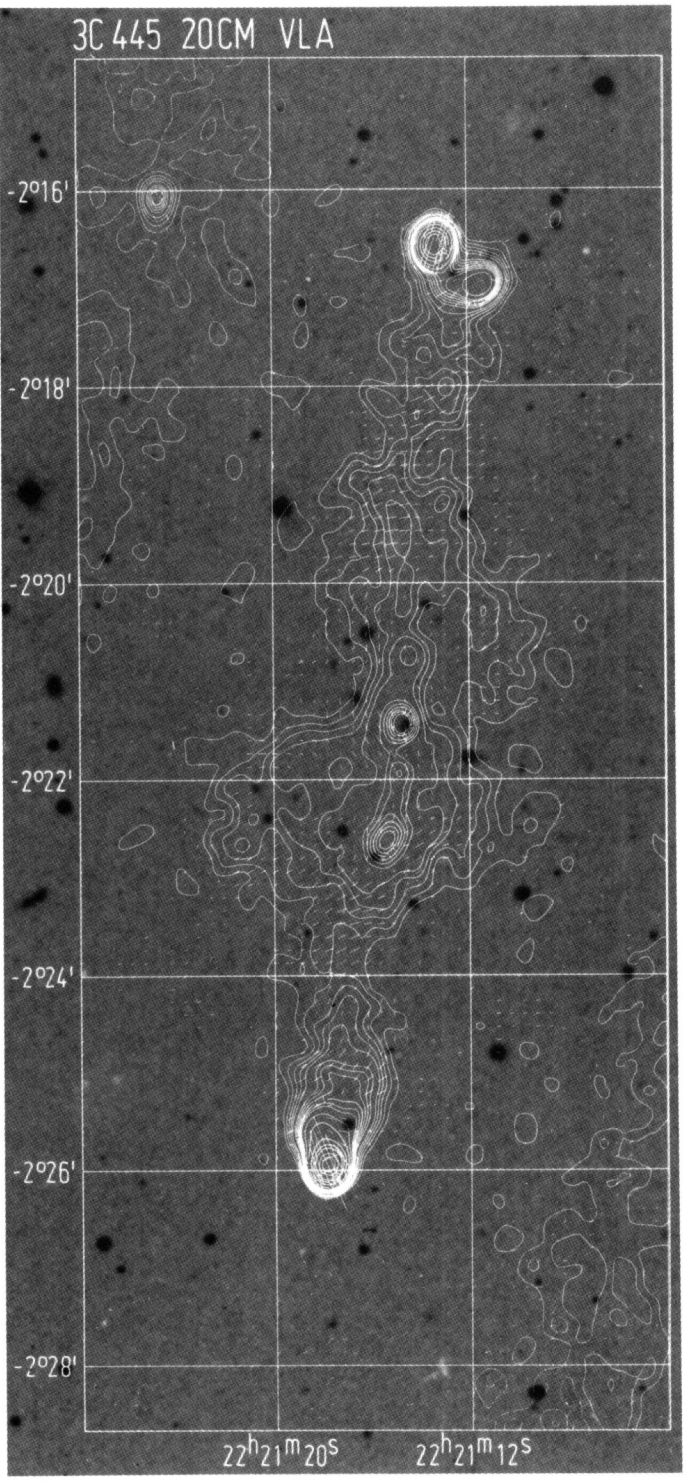

Fig. 5. Continuum $\lambda 21$ cm map of 3C 445 superimposed on the optical field from the Palomar Sky Atlas Survey. Contours are shown at 5, 10, 15, 20, 25, 35, 40, 45, 50, 55, 60, 75, 100, 150, 200, 250, 350, and 425 mJy/beam. The polarization intensities are scaled such that 1 arc minute equivalent length corresponds to 83 mJy/beam

3.2.1. Polarization and rotation measure in 3C 445

The Effelsberg $\lambda 2.8$ cm map of 3C 445 is shown in Fig. 6, which also shows the distribution of polarized intensity and position angle. Since the integrated rotation measure of 3C 445 is only $+12\,\mathrm{rad\,m^{-2}}$ (which corresponds to a rotation of 28° between $\lambda\lambda 2.8$ and 20.5 cm) we assume that, at the common resolution of 75″, any differential Faraday rotation is less than 180°. The rotation measure distribution is shown as a contour plot in Fig. 7. There are no strong RM variations over the source; the RM varies between $+15$ and $0\,\mathrm{rad\,m^{-2}}$ in the northern half of the source, and between -10 and $+10\,\mathrm{rad\,m^{-2}}$ in the southern half. The systematically lower RM in the region of the southern, highly polarized bridge is the most interesting feature of this distribution, although it cannot be unambiguously separated from small-scale galactic RM variations. Also, small-scale changes in intrinsic polarization direction, possibly combined with rapid spectral index changes over our 75″ beam could produce apparent changes in RM. We can nonetheless use the RM distribution in Fig. 7 to establish limits to systematic large-scale changes in RM within or around the source. The average foreground galactic RM can be estimated from the RM's of 5 nearby sources, whose average RM is $-10\pm 11\,\mathrm{rad\,m^{-2}}$. This correction would add $\sim +10\,\mathrm{rad\,m^{-2}}$ to the values in Fig. 7, although this is somewhat uncertain given the standard deviation of $11\,\mathrm{rad\,m^{-2}}$.

The $\lambda 2.8$ cm polarization vectors are very close to the intrinsic E-vector directions (Fig. 6), and show that the prevailing magnetic field direction is *along* the radio bridges over a distance of ~2′.5 (~152 kpc), and beginning at most ~30 kpc behind each outer head. The polarization degree is typically 12–30 % at 2.8 cm in these zones, which, as can be seen in Fig. 5 (the full resolution 20 cm map) are quite narrow, and not completely resolved in the transverse direction with the 12″ VLA beam. Examination of the 20 cm map suggests that the lower percentage of polarization at 2.8 cm in the inner bridges is due to beamwidth smearing of small-scale changes in position angle. The intrinsic polarization degree at 20 cm is still locally high in some areas here.

3.2.2. Spectral index variations

Comparison with the smoothed (down to 75″ HPBW) 20 cm VLA map (Fig. 5) shows a striking difference in the "bridge" emission, which is noticeably wider at 20 cm. In fact the spectrum of the outer "sides" of the bridge is so steep that no emission is detectable here in our 2.8 cm map (Fig. 6). This suggests that the outer, steep spectrum population of electrons in the outer portions of the bridge have travelled away from the source axis without being re-accelerated. The transport away from the source axis may also be associated with "backflow" from the outer heads. The entire range of spectral index cannot be measured, since this resolution probably smears out smaller scale variations.

In contrast to spectral index variations transverse to the axis of 3C 445, there are *no large-scale spectral index variations along the source* axis which are apparent at the common resolution of 75″. This suggests that particles are continuously, or quasi-continuously accelerated over the projected 0.3 Mpc distance from the galaxy center. By the same token, our discovery of marked spectral index steepening transverse to the radio axis suggests that there is no acceleration off the radio source axis. This is an interesting result, which supports the model of collimated energy flow over megaparsec scales in extended extragalactic radio sources.

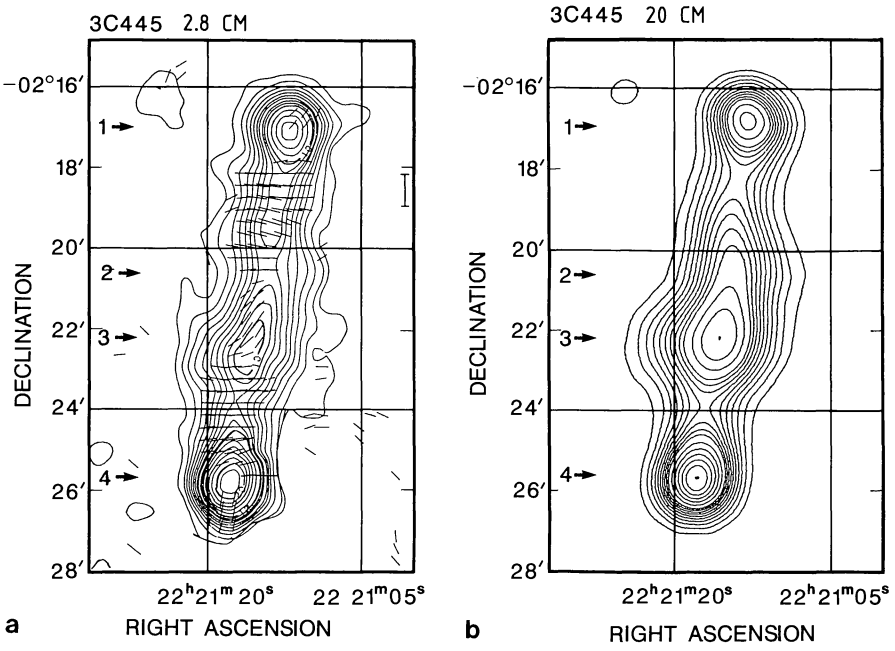

Fig. 6. **a** Radio map of the total intensity of 3C445 at $\lambda 2.8$ cm, mapped by the Effelsberg 100-m telescope. The HPBW is 75″. Contours are shown at 10, 20, 30, 40, 50, 60, 70, 80, 90, 100, 120, 140, 160, 180, 200, and 220 mJy/beam. The linear polarization lines (maximum E-vector plane) are scaled such that 1 arc minute-equivalent length corresponds to 26.8 mJy/beam. **b** Smoothed 20 cm VLA map showing the broadening of emission in sections marked with 2 and 3

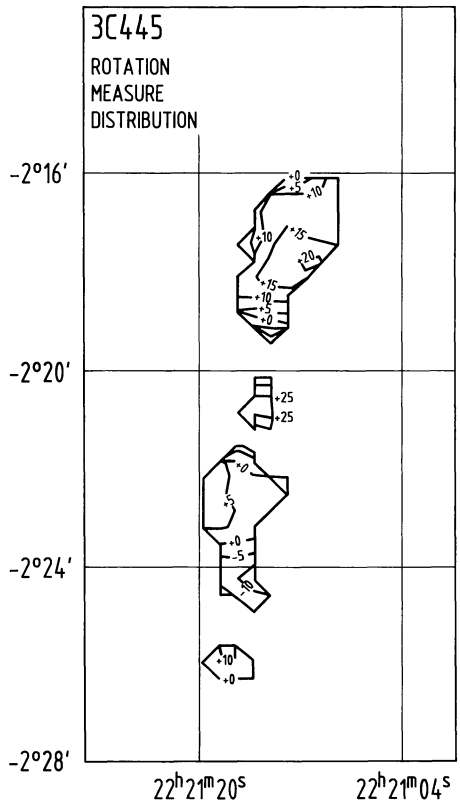

Fig. 7. Distribution of the Faraday rotation measure over 3C445 at 75″ resolution between $\lambda\lambda 2.8$ cm and 20 cm

4. Inference of the relativistic gas properties from analysis of the morphology, surface brightness, spectral steepening, and rotation measure

In the following, we shall explore which parameters of the radio system can be deduced, or limited, given the polarization and spectral index variations in 3C445.

We assume that continuous acceleration of the relativistic gas occurs only along the energy pipeline between the galaxy nucleus and the outer hotspots. In the case of 3C445, the following inferences and measurements can be made from our radio maps at 1.46, 4.8, 10.6, and 15 GHz:

(1) We can estimate the synchrotron volume emissivity, of the well-resolved, "relaxed" inner bulge, and calculate its minimum energy density, u_s, (assuming equipartition), hence minimum pressure. The assumption of equipartition gives a magnetic field strength

$$u_s = 7.9 \times 10^3 (1+k)^{4/7} L^{4/7} R^{-12/7} \text{ erg cm}^{-3} \quad (1)$$

and

$$H_{\text{eq}} = 2.8 (1+k)^{2/7} R^{-6/7} L^{2/7} \text{ Gauss}, \quad (2)$$

where k is the ratio of relativistic proton to electron energy, L the radio luminosity (erg/s) of the region with characteristic radius R(cm) (cf. Pacholczyk, 1970), and $H_{\text{eq}(0)}$ is the equipartition magnetic field for $k = 0$.

(2) We can equate u_s in the bulge to the energy density of the ambient IGM, u_{ig}, with which it is assumed to be in approximate pressure equilibrium.

$$u_s \cong \frac{3}{2} n_{ig} k T \text{ erg cm}^{-3}. \quad (3)$$

(3) The distance from the jet axis to the measured point of spectral steepening tells us how far relativistic electrons of a given energy have been transported off axis (we assume without reaccelertion, and perpendicular to the jet axis) before they lose

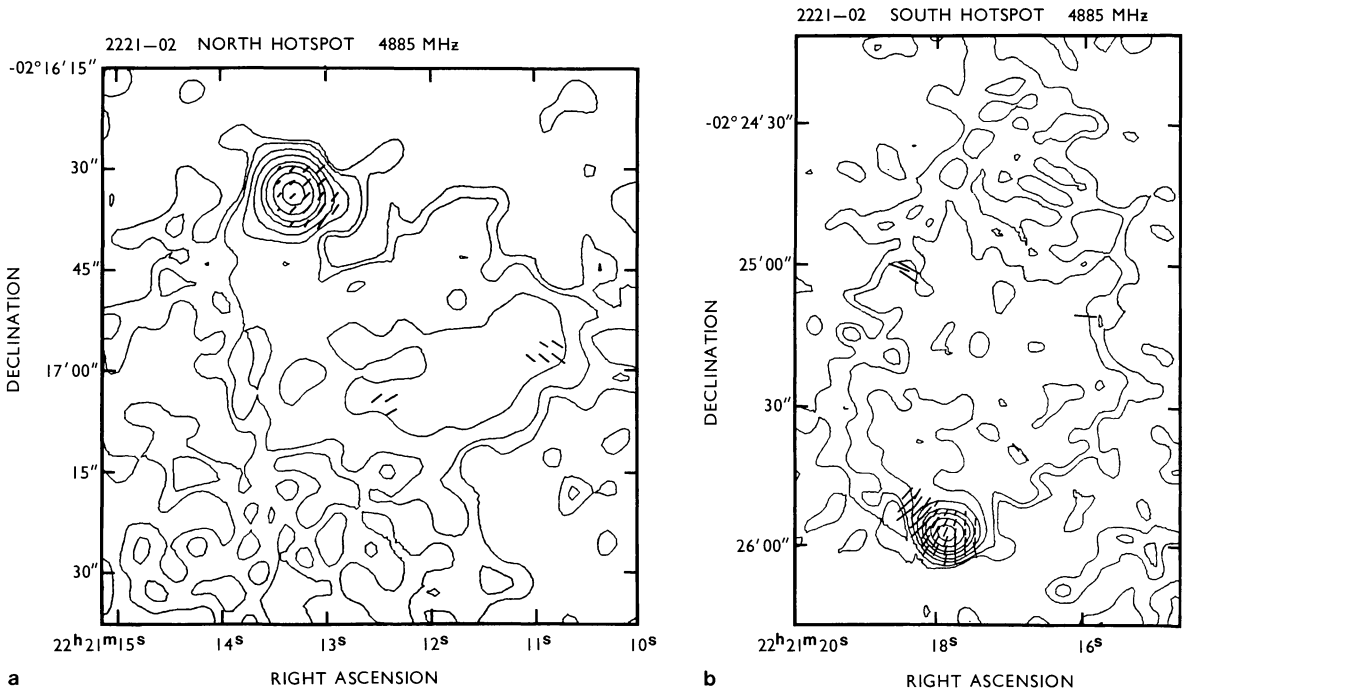

Fig. 8. **a** 4885 MHz map of the northern hotspot of 3C 445 (2221-02) having a HPBW of 4.5. Contours are shown at 1, 2, 5, 10, 20, 30, 50, and 80% of peak surface brightness, which is 89.5 mJy/beam. The polarization lines are proportional to degree of polarization and are scaled such that 1″ equivalent length =22.4%. The westward extension of the hotspot is ~35% polarized. **b** Corresponding 4885 MHz map of the southern hotspot whose contours are scaled as in **a** to the peak surface brightness of 118 mJy/beam. The percent polarizations are scaled such that one arcsecond equivalent length corresponds to 11.0%. The degree of polarization peaks towards the opposite side from the northern hotspot, at a value of ~35%

their energy. The magnetic field strength derived in (2) gives a corresponding loss time

$$\tau = 32\, \nu_m^{-1/2}\, H_{\mathrm{eq}(0)}^{-3/2}\, (1+k)^{-3/7}\, \mathrm{yr}, \tag{4}$$

where ν_m is the frequency of the spectral turnover at some distance D_t from the source axis and $H_{\mathrm{eq}(0)}$ is the magnetic field strength for $k=0$. The distance at which the 10.6 GHz loss turnover is difficult to quantify precisely, since the resoloution common to 1.46 and 10.6 GHz was only just sufficient to establish this effect. One should ideally have comparable maps at one or two additional frequencies in order to better verify the variation of turnover frequency with distance from the source axis. In the absence of such detailed "spectral index map", we must content ourselves with a very crude estimate of $D_t = 6\ 10^4$ pc, at which electrons cease to radiate at 10.6 GHz.

This distance, estimated from measurement, divided by the loss time gives a transverse transport speed, V_t

$$V_t = \frac{D_t}{\tau} \approx 1230\ (1+k)^{3/7}\ \mathrm{km\,s^{-1}}. \tag{5}$$

We can compare V_t with the estimated sound velocity in the ambient IGM

$$V_s = \left(\frac{\gamma k T}{\mu m_H}\right)^{1/2} \approx 452\ \sqrt{T_7}\ \mathrm{km\,s^{-1}}, \tag{6}$$

where T_7 is the IGM temperature in units of 10^7 K and μ is the mean ion mass. The two velocities are comparable when $T \sim 10^8$ K, provided k is not very large. We note here that if k were of order 100 or greater, then $V_t/V_s \geqq 6$ at 10^8 K, which would require that the bulge should be expanding supersonically sideways. This is at variance with the relaxed appearance of the inner bulge, and argues for values of the relativistic proton/electron energy ratio which are $\ll 100$.

(4) The outer heads, having a different internal energy density, u_b, and which we have not yet considered, are assumed to be in ram pressure equilibrium with the IGM, into which they are advancing with velocity V_b:

$$u_b = u_{ig} + \varrho\, V_b^2. \tag{7}$$

From the measured 15 GHz surface brightness, we estimate the value of u_b to be $1.3\ 10^{-10}\ (1+k)^{4/7}\ \mathrm{erg\,s^{-1}\,cm^3}$, whereas $u_{ig} \sim u(\mathrm{bridge}) = 1.06\ 10^{-12}$. Since the external sound speed can also be expressed as $V_s = (u_{ig})^{1/2}$ we can write

$$\frac{V_b}{V_s} = \sqrt{\frac{u_b}{u_{ig}}} - 1. \tag{8}$$

The ratio, $u_b/u_{ig} \sim 123$, which gives a Mach number (M) of ~11. This is a minimum in the sense that M will increase if $k > 1$. Since $u_b \gg u_{ig}$, the temperature of the ambient medium becomes unimportant in the ram-pressure dynamics. The velocity of the outer blobs of 3C 445 can be estimated as:

$$V_b \approx \frac{2000\,(1+k)^{2/7}}{(n_{-3})^{1/2}}\ \mathrm{km\,s^{-1}}. \tag{9}$$

We can now combine (5) and (9) to get the ratio V_t/V_b, which is close to another observable – namely the width/length ratio (W/L) of 3C 445

$$\frac{V_t}{V_b} \approx 0.6\ n_{ig-3}^{1/2} (1+k)^{1/7}, \tag{10}$$

where n_{-3} is the electron density in units of 10^{-3} cm^{-3} of the IGM surrounding the outer head. It is useful to re-arrange (9) as follows:

$$(1+k) \cong 30\, n_{ig\,-3}^{-7/2} \left(\frac{V_t}{V_b}\right). \quad (11)$$

We assume that V_t and V_b have been constant with time as the radio source expanded, and in any case it is reasonable to expect that $V_t/V_b < 1$. This gives a constraint on k for any reasonable value of n – which can also be tied to the observed limits on differential Faraday rotation (see below). Furthermore, relation (11) shows that a given V_t/V_b implies an *upper limit* for n_{-3}, which corresponds to the case where $k = 0$. Taking $V_t/V_b = W/L \sim 4/13$ for 3C 445, we deduce that n_{-3} cannot be greater than 0.25, given the assumptions stated earlier.

(5) The RM map of 3C 445 shows that the RM difference between the lobes is ~ 10 rad m^{-2}. From this datum we can reasonably infer that the ambient gas surrounding the entire source does not generate a Faraday rotation which is more than this over dimensions of $\sim 1' = 60$ kpc. This sets a limit on $n_{ig} \cdot H_{ig}$

$$n_{ig} \cdot H_{ig} < 2\ 10^{-10}\ \text{cm}^{-3}\ \text{G} \quad (12)$$

assuming a value of $\sim 1\,\mu$G for the H_{ig}. Allowing for field reversals, the low differential Faraday rotation around 3C 445 leads to an upper limit; $n_{ig} \lesssim 2\ 10^{-4}$ cm^{-3}.

In all of the foregoing discussion it is assumed that the k-factor, and ambient IGM density are the same for both bulge and outer heads of 3C 445. The respective values of n_{ig} could be radially scaled according to the expected gas density distribution around the parent radio galaxy, however, the level of detail in the present observations of 3C 445 do not warrant this refinement here.

For the various assumptions in (1)–(5), it is possible to deduce both n_{ig} and the relativistic proton/electron energy ratio (k). Combining (6), (8), and (11), taking $T_7 = 10$, and $V_t/V_h \sim W/L = 4/13$ (cf. Figs. 5 and 6), we obtain the following results:

$k \sim 5$

$n_{ig} \sim 1.5\ 10^{-4}$ cm^{-3}.

For this combination of parameters, the outer head's velocity, V_h, is highly supersonic, as it should be for effective ram pressure confinement, whereas V_t is only slightly above the sound speed which is close to the assumption in (3) of quasi-static confinement of the bulge. Also, n_{ig} is just below the upper limit required by relation (12) and its assumptions. For $T = 2\ 10^8$ K, the values become:

$k \sim 13$

$n_{ig} \geqq 1.2\ 10^{-4}$ cm^{-3}.

The trends of these numbers with varying temperature show, for the set of assumptions we have adopted, that the ambient IGM density is difficult to reduce substantially below 10^{-4} cm^{-3} without extremely high *IGM temperatures*, and the relativistic proton/electron ratio is of order 5–20, rather than 1 or 100. Also, the ambient IGM temperature must be $\gg 10^7$ K to avoid an implausibly large *IGM density* and, in particular, to be consistent with the very small differential RM across the 0.6 Mpc projected size of the radio source.

5. Conclusions

Our multi-frequency radio maps of 0634-20 and 3C 445 show several interesting morphological features. In particular both possess a large degree of symmetry in their overall structure, and highly ordered, parallel-oriented magnetic fields just inside the outer heads, where the transverse dimensions of both sources are smallest.

Faraday rotation maps of high sensitivity show very little variation of RM over the sources. Their 15′ and 10′ angular sizes have enabled us to use them as two of the first sensitive probes of arc-minute scale variations of the foreground galactic RM. For 0634-20, which lies in a zone of moderately large galactic RM, we are able to set upper limits on the *precentage* change of the interstellar RM over scales up to 15′ in that direction ($l = 230°$, $b = -12°$).

The large frequency baseline, high resolution and good sensitivity afforded by the combination of the Effelsberg 100-m telescope and the VLA enable us to verify that 3C 445 steepens its spectral index away from the source axis in its central bulges. By contrast, there is little large-scale variation of spectral index along the outer components of either of these giant radio sources.

We show how a quantitative analysis of 3C 445, combined with some basic physical assumptions which appear consistent with its morphology, lead to estimates of the relativistic k-factor, and the ambient IGM density and temperature. Under our set of assumptions, k is in the range 5–20, $T \sim 10^8$ K, and the IGM density is of order 10^{-4} cm^{-3}.

Acknowledgements. We thank C.J. Salter, U. Klein, L. Fenton-Lloyd, and L. Carriere for their assistance with the data reduction, and R.N. Henriksen and U. Klein for discussions. We are grateful to the Director and Staff of the NRAO for VLA observing time and for their support. This project was supported in part by the Natural Sciences and Engineering Research Council of Canada (NSERC).

References

Danziger, I.J., Goss, W.M., Frater, R.H.: 1978, *Monthly Notices Roy. Astron. Soc.* **184**, 341

Emerson, D.T., Klein, U., Haslam, C.G.T.: 1979, *Astron. Astrophys.* **76**, 92

Fosbury, R.A.E., Tadhunter, C.N., Bland, J., Danziger, I.J.: 1984, *Monthly Notices Roy. Astron. Soc.* **208**, 955

Klein, U., Emerson, D.T.: 1981, *Astron. Astrophys.* **94**, 29

Pacholczyk, A.: 1970, *Radio Astrophysics*, W.H. Freeman

Rudy, R.J., Tokunaka, A.T.: 1982, *Astrophys. J.* **256**, L1

Schilizzi, R.T., McAdam, W.B.: 1975, *Memoirs Roy. Astron. Soc.* **79**, 1

Simard-Normandin, M., Kronberg, P.P., Button, S.: 1981, *Astrophys. J. Supl.* **45**, 97